INTERNATIONAL JOURNAL OF RECENT TRENDS IN ENGINEERING & RESEARCH
Impact Factor 4.101 ISSN -2455-1457
RECENT ADVANCES IN ELECTRONICS & COMMUNICATION ENGINEERING (RAECE-2K17)

Design of Printed Transducers for Organic Coating of Metalic Substrates Using Capacitive Touch Sensors

P.S.Sreenivasa Reddy[1]
Associate Professor(ECE)
Nalla Narsimha Reddy Engg. College, Hyderabad, Telangana, India

B.Suneetha[2]
Associate Professor(ECE)
Nalla Narsimha Reddy Engg. College, Hyderabad, Telangana, India

***Abstract*—We present the first realization of printed capacitive touch buttons and touch pads integrated into the organic coatings on sheet steel. The properties of coated sheet steel relevant for printing are discussed and compared with substrates, commonly used for printed electronics. Different designs and read-out methods for capacitive buttons on sheet steel have been screen printed and their sensitivity in dependence on design parameters is rated.**

***Index Terms*—Organic coating, embedded transducer, embedded sensor, conductive substrate, capacitive button, rough surface, substrates for printed electronics.**

I. INTRODUCTION

We present the first realization of printed capacitive touch buttons and touch pads integrated into the organic coatings on sheet steel. Remarkable progress has been made in recent years in the field of printed electronics mostly on flexible substrates. The basis for this development is the large number of low temperature (i.e., temperatures below 200°C) curable conductive inks, including nanoparticle or flake based silver [1], gold [2], nickel [3] and copper inks [4], particle free reactive silver inks [5], silver nanowire inks [6], carbon [7] and conductive polymers [8] based inks, which have been developed in recent years. Many similar inks are available commercially today. Numerous electronic structures, which required cost-intensive semiconductor fabrication processes in the past, can now be printed, like, e.g., OLEDs [9], electro chromic displays [10], RFID tags [11] and polymer solar cells [12]. In general, these structures are printed on polymeric foil, glass or coated paper.

In contrast to these substrates, sheet steel features a comparatively rough surface which impedes the realization of embedded electronics. Furthermore, spurious capacitances are large due to low thickness of the isolating layer (~10 µm). In this contribution, the surface properties of coated sheet steel are compared to commonly used paper and plastic substrates. Furthermore, the integration of capacitive and resistive structures into the organic coatings of sheet steel, which we consider as a basis for the integration of more complex functionality, is presented and the influence of top coat and electrode thickness (which can be neglected in traditional capacitive sensors) on touch sensor sensitivity is examined.

II. TECHNOLOGICAL CONSIDERATIONS:COATED STEEL AS SUBSTRATE

From all surfaces one may want to print electronics on, coated sheet steel is supposedly among the most challenging. It is rough, the coating cannot withstand high curing temperatures, and the isolating layer is thin, which results in high spurious capacitances. Nevertheless, it also offers some unique advantages. First, it is roll-to-roll compatible, i.e., electronic structures can be produced with little extra cost. Second, the sheet steel is self-supporting, i.e., it can be designed to be, e.g., part of a housing (of electronic devices) or a facade panel. Furthermore, the electronic structures are intrinsically integrated, no further assembly is required. In the following we discuss the suitability of the steel substrate by characterizing it in terms of surface roughness and compatibility of the inks and pastes to be applied.

2.1. Surface Roughness

The surfaces of sheet steel samples, coated with polyester (Primer 1) and polyurethane (Primer 2) primer respectively, were characterized with a Bruker DektakXT surface profiler (see Fig. 1) in terms of arithmetical mean

deviation *Ra*, the rms deviation *Rq* and the average maxim height *Rz* of the profile, using ISO 4287 [13]. Throughout this work, the primer coatings were applied with a Mayer rod and were thermally cured before further use. The waviness of the profile was removed with a Gaussian high pass-filter with a cut-off wave-length of 0.8 mm. To rate the obtained parameters, the surfaces of various paper substrates were analyzed as well; results can be found in Table I. The surface parameters of the two primers are in the same range.

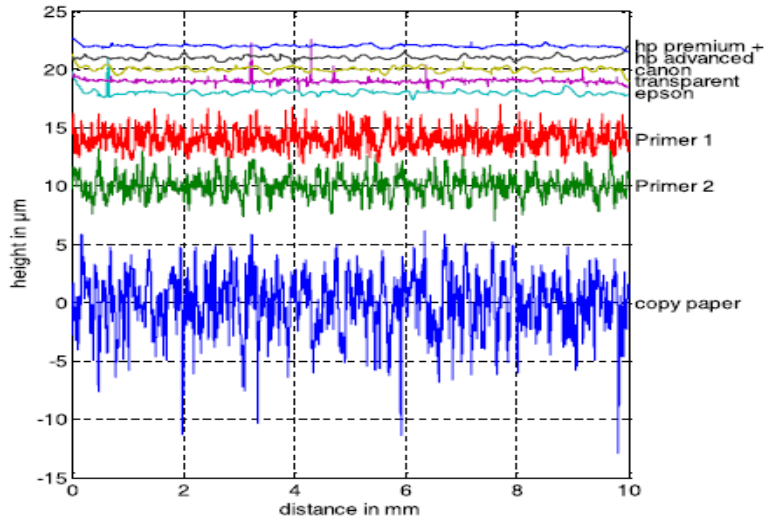

Fig.1. Surface profile of organic primers and a selection of paper substrates, recorded with a Bruker DektakXT surface profiler. The profiles are filtered to remove the waviness of the substrate.

	Ra/µm	*Rq/µm*	*Rz/µm*
Copy paper (80g/m²)	2.0	2.5	12.6
Primer	0.7	0.9	4.0 – 5.0
Photo paper	0.1-0.2	0.1-0.2	0.4-.9
PET	0.002 [8] 0.01 [2]	-	0.014 [8]
Glass	-	0.001[9]	-
Paper (other authors)	-	0.5-20 [6]	-

TABLE I
SURFACE PARAMETERS OF SAMPLES, CHARACTERIZEDWITH THE SURFACE PROFILER. FURTHERMORE, SURFACE PARAMETERS OF PET AND GLASS, WHICH ARE COMMONLY USED FOR PRINTED ELECTRONICS, TAKEN FROM LITERATURE, ARE GIVEN.

In comparison to plastic foils (which show *Ra* values in the lower nm range [14], [15]) and coated paper, the organic primers are rough. The high surface roughness impedes the printing of very thin conductive layers and excludes certain applications of printed electronics, like, e.g., OLEDs, which require homogeneous, defect free layers with well-defined thicknesses. Uncoated paper, in general, is rougher than the organic primer layer. Despite of its rough surface, many applications, including light-emitting electrochemical cells [16] and loudspeakers [17], have been realized on uncoated paper. Further examples for printed electronics on paper are given in [18]. For printed electronics on coated sheet steel, we expect a similar range of applications.

2.2. Ink Compatibility

Important ink parameters to be considered for printing on organic coatings are the surface tension, curing time and temperature, and the solvent resistance. Furthermore, the ink viscosity and solvent evaporation rate has to be adjusted to the printing process.

The surface tension of the inks and the surface energy of the substrate, which is in the range of 37 mN m^{-1} (polyarylate) and 42 mN m−1 (PET, Kepton) [19] for plastic foils and 28 mN m^{-1} – 33 mNm^{-1} for our organic coatings, are crucial for the printing process. To obtain good printing quality, the two parameters do not have to be totally equal but if the surface energy of the substrate is much smaller than the surface tension of the ink, bulges will occur [19]. In the opposite case, the printed features will suffer from wetting. Furthermore, when a top coat is applied, the surface energy of the printed structure is crucial for adhesion and durability. A printed feature and successively applied top coat may optically appear flawless, but blistering due to insufficient adhesion may still appear (see Fig. 3). Commercially available inks are often optimized for printing on commonly used plastic substrates, i.e., the surface tension might not be suitable for printing on organic coatings. Wetting of the primer, e.g., can be enhanced by addition of surfactants to the ink or by heating of the substrate. In an ink jet process, we used a nanoparticle based silver ink with triethlyene glycol monomethyl ether (TEGME) as solvent (Sigma-Adrich).

Without heating of the substrate, the wetting of the surface is insufficient, droplets form, but with heating well defined structures can be printed.

Furthermore, chemical resistance of the organic coating to the ink's solvent is crucial. This problem also can be reduced by heating. TEGME is a solvent with a high boiling point and can attack the organic primer if contact time is too long. By heating, the evaporation rate of the solvent increases and the printed pattern is dried before the surface suffers damage. A more general solution to the problem is to ensure that the solvent of the ink does not dissolve the coating. If solubility parameters [20] of the coating and ink differ significantly (i.e., the solubility parameters of the solvent are outside the solubility sphere of the coating), then the coating will not be dissolved. Often, the solubility parameters of the coating are not available. In this case, the solubility parameters of the coating's solvent could be a good estimate.

III. PROCESS CONSIDERATIONS: PRINTING ON COATED SHEET STEEL

Screen and inkjet printing are currently being used to realize capacitive and resistive structures on coated sheet steel. Inkjet printing is performed with a drop-on-demand printer (micro drop Technologies). The nozzle of the piezoelectric print head features a nozzle diameter of 70 µm. The typical surface profile of a capacitive sensor, printed with silver nanoparticle ink is depicted in Fig. 2. The position of the traces can be identified visually, determining their height, however, is not possible. We estimated that it is in the range of the average surface roughness *Ra*. Despite the low conductor height and the roughness of the surface, good electrical conductivity is reached, the sheet resistance *R*s is in the order of 0.5 Ω (i.e., a factor 2-5 worse than estimated from the bulk conductivity, specified for the ink). The substrate was heated to 80 °C before printing to enhance wet ability and solvent evaporation.

Screen printing was used when thicker conductors are needed or acceptable. In general, the printing thickness can be adjusted (in a limited range) by the mesh of the screen. Typical conductor thicknesses achieved with silver pastes and mesh sized used in this work are ranging from 3 µm to 6 µm. Limits for the thickness of the conductor are given by the thickness of the later applied top coat, as embedded conductors, in general, must not influence the waviness of the top coat. Furthermore, flexibility of the conductor has to be maintained, it should at least be as durable to deformation as the coating system.

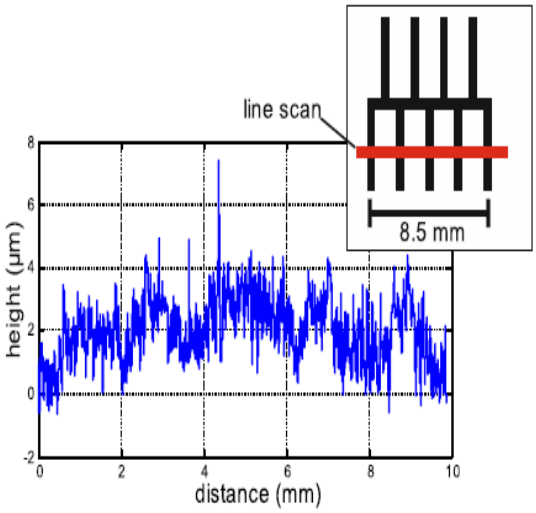

Fig.2. Surface profile of an ink-jet printed capacitive sensor (8.5 mm × 8.5 mm), measured over five fingers of the sensor.

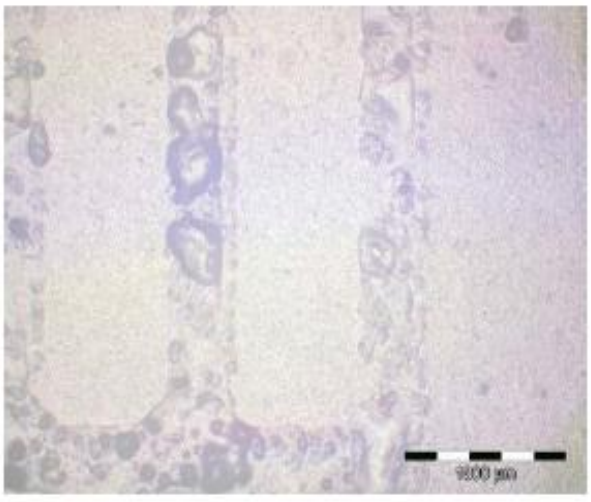

Fig.3. Blistering of a top coat, observed after being exposed to an accelerated test environment (QCT condensation tester) for several weeks.

IV. DESIGN CONSIDERATIONS

Capacitive touch buttons and a multilayer touchpad are presented exemplarily in this contribution. Touch buttons relying on measurement of the self or mutual capacitance were fabricated.

4.1. Influence of Coating Thickness

The sensitivity of these buttons in dependence on the thickness of an applied top coat and on the thickness of the primer layer is investigated. The primer layers were applied on the sheet steel substrate with a Mayer rod and thermally cured before further use. The capacitive elements, which can be seen in Fig. 4, were screen printed, using

a manual screen printing machine, with a silver nanoparticle based ink (InkTecTEC-PA-010) on polyester based primers with 6 µm and 20 µm thickness. A printed line thickness between 3 µm and 4 µm was achieved with a screen mesh of 140 treads/cm.

The line thickness was measured with a Dektak XT profilometer. After annealing at 140 °C for 10 minutes, polyester based top coat layers with thicknesses ranging from 9 µm to 27 µm were spin coated over the sensors. The top coat was cured on a 260 °C hot plate for 90 s and immediately quenched in water afterwards.

The sensors are 10 mm long and 8 mm wide. The conductive area of both sensors is equal to provide a better comparability between the sensors. This is reached by implementing a grid structure with an opening of 1.2 mm x 1.0 mm into the self capacitance sensors. The width of the gaps and the tines of the mutual capacitance sensor is 0.45 mm. As reference and to investigate the influence of conductor thickness, thermally evaporated gold buttons with a thickness of 50 nm were fabricated on the same type of substrate (i.e., polyester based primer on sheet steel) as well.

With a self-capacitance based sensor, the capacitance between electrode and grounded substrate is considered (see Fig. 4a). In contrast, a mutual capacitance sensor is based on the capacitive coupling between two electrodes (see Fig. 4b). To enhance the coupling, sensors based on mutual capacitance are often designed with interdigitated electrodes or, if applied on different layers, shifted to each other (e.g., diamond shaped touchpad). To reduce the offset which would be introduced by the sensor's self-capacitance, the substrate is grounded during the measurement of the mutual capacitance.

The influence of a standard finger (the author's) on the mutual and on the self-capacitance of the printed elements was measured with an Agilent 4294A impedance analyzer in the frequency range between 1 kHz and 1 MHz. The sensor capacitances were extracted by fitting the complex data to a *RC* circuit. While measuring the mutual capacitance, the steel substrate was connected to ground. As shown in Fig. 6, the change of the self-capacitance does not depend on the primer thickness (in contrast to the base capacitance, which can be approximated by a plate capacitor). The base mutual capacitance C_0 (i.e., the mutual capacitance without user interaction), which is in the range of 6 pF, is not significantly influenced by the primer or the topcoat thickness. The sensitivity S of the buttons is rated by $S = C/C_0$, where C is the mutual capacitance which is obtained when a finger is placed on the sensor (see Fig. 5). In general, the mutual capacitance based buttons are more sensitive to user interaction than the self capacitance based. This can be attributed to their low base capacitance.

Primer thickness and conductor thickness affect the sensitivity of the mutual capacitance based buttons; thicker primer and thicker conductor results in higher sensitivity. The sensitivity of self-capacitance based buttons in mainly affected by the primer thickness, no significant influence of the conductor thickness was observed.

4.2. Mutual Capacitance: Influence of Electrode Width and Spacing

The sensitivity of mutual capacitance based sensors on the gap width between electrodes and on the electrode width was investigated. Sensors with different electrode and gap width were screen printed on top of a 20 µm thick polyester based primer and afterwards spin coated with a 17 µm thick polyester based top coat layer. Screen printing was conducted with two silver inks, a nanoparticle based ink (InkTekPA-010) and a silver flake based ink (Henkel Electrodag PF-050). For both inks the same printing screen with 150 threads/cm was used. The difference of the inks can be seen in the height of the printed electrodes. Electrodes printed with PA10 were between 2 µm and 3 µm thick. With PF-050, a height between 4 µm and 5 µm was reached. The sensor dimensions are given in TABLE II.

The influence of an interaction with 500 µL deionisied water and with a finger on the mutual capacitance was recorded with an Agilent 4294A impedance analyzer. During the measurement, the steel substrate was connected to ground. The capacitive behavior of a sensors is given by $C_p(\omega) = \Im(Y)/\omega$. Exemplary, the response of sensors printed with PF-050 is depicted in Fig. 7. When interacting with water, a strong frequency dependence of the sensor's mutual capacitance can be seen. The mutual capacitance, influenced by a finger, is (almost) constant over the considered frequency range.

The sensor interaction with water is evaluated in the high (1 MHz) and low (1 kHz) frequency limit. Its dependence on gap (and electrode) width is depicted in Fig. 8. In the low frequency limit, the change of the mutual capacitance is approximately three times larger than in the high frequency limit. The influence of the finger on the mutual capacitance decreases with increasing gap width.

The frequency dependence can be explained by considering the equivalent circuit model of the mutual capacitance sensor in contact with an interacting media (see Fig. 9). Each of the sensor electrodes couples capacitively to ground
(C_{1G} and C_{2G}) and through the top coat layer (C_{1T} and C_{2T}) to the surface. The coupling between surfaces through a contacting media is described by a *RC* circuit (R_m and C_m). Due to the proximity to the conductive steel substrate, coupling from the media to the substrate (modeled by C_{TG}) occurs. To model the exact impedance behavior of water,

in general, more complex equivalent circuit models are required. A more advanced model can, e.g., be found in [21]. However, as will be shown in the following, the *RC* circuit is appropriate to explain the frequency behavior of the sensor.

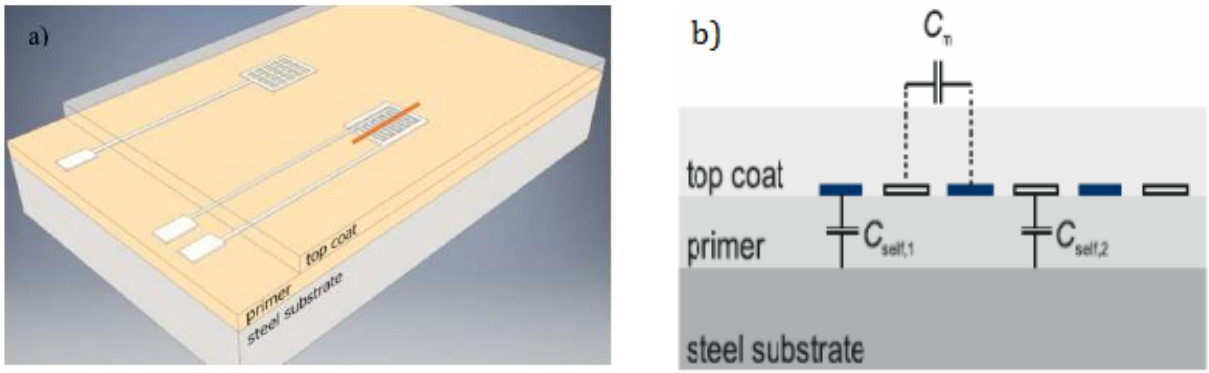

Fig.4. a) Schematic layout of self (upper) and mutual (lower) capacitance based buttons. (b) Cross section of a mutual capacitance based button with capacitive coupling schemas.

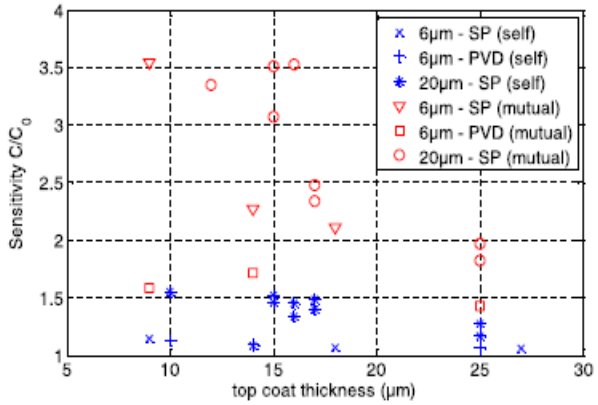

Fig.5. Sensitivity of the printed buttons to user interaction (SP: screen printed; PVD: thermally evaporated gold electrode).

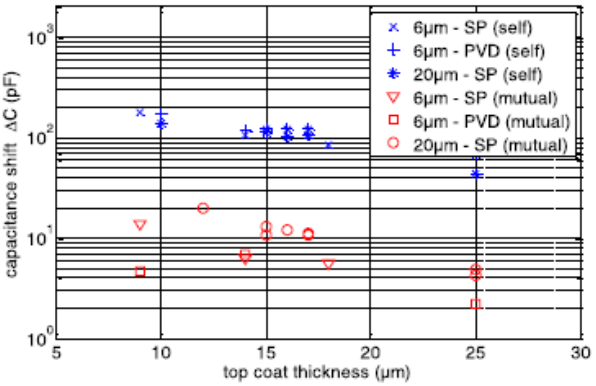

Fig.6. Influence of a standard finger on the capacitance of self- and mutual capacitance based buttons (SP: screen printed; PVD: thermally evaporated gold electrode).

Assuming that the sensor output (i_{out}) is connected to virtual ground, the current i_{out} is given by

$$i_{out} = \frac{u_{in}}{\left(\frac{1}{Y_{2T}} + \frac{1}{Y_m}\right)\left(\frac{1}{\frac{1}{Y_{2T}}+\frac{1}{Y_m}} + Y_{TG}\right)\left(\frac{1}{Y_{1T}} + \frac{1}{Y_m} + \frac{1}{Y_{2T}+Y_{TG}}\right)}, \quad (1)$$

where Y_x is the admittance of part x. The mutual capacitance C_{21} of the sensor can then be defined by

$$\Im(i_{out}) = \omega C_{21} u_{in}. \quad (2)$$

For the given sensor dimensions the influence of *R*m can be neglected at low frequencies compared to C_{1T}, C_{2T} and C_{TG}. Using this assumption, a simplified relation for C_{21} can be obtained:

$$C_{21} = \frac{C_{1T}C_{2T}}{C_{1T} + C_{2T} + C_{TG}} \quad (3)$$

Note that, if the resistors *R*m cannot be neglected, the mutual capacitance defined according to (2) becomes frequency dependent. In a simple model, C_{1T}, C_{2T} and C_{TG} are approximated as plate type capacitors. The surface area of C_{1T}, C_{2T} are given by the area of the individual electrodes, the area of C_{TG} is defined by the drop area A_{drop} minus the electrode areas (compare Fig. 10). Using this model, an excellent agreement between the estimated "low frequency" mutual capacitance and model can be found (compare Fig. 8). The result has to be reviewed with care as small measurement errors of electrode height or coating thickness would change the slope of the model drastically. To cross-check the plausibility, 2D simulations of the structure were performed and the agreement between simulated and the modelled results is considered. This topic will be further discussed in the next section.

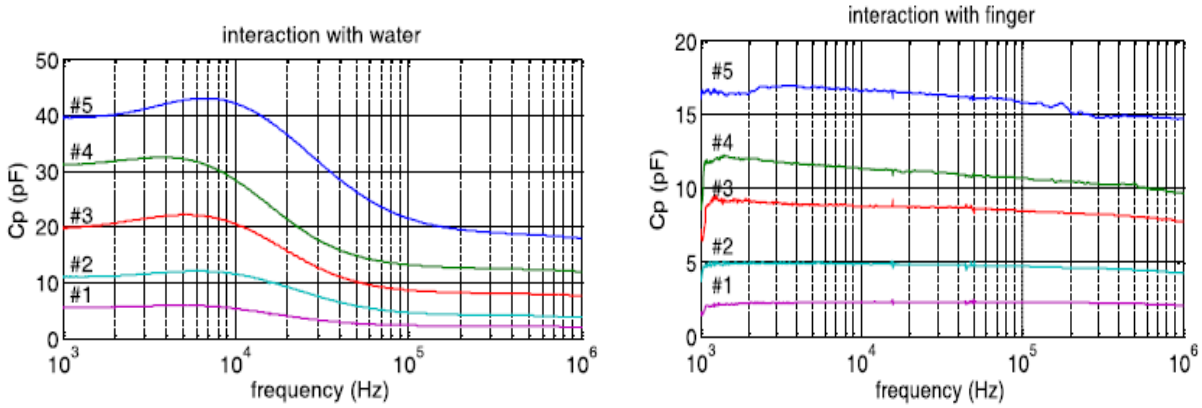

Fig.7. Frequency dependence of the mutual capacitance of sensors printed with PF-050 in contact with a drop of water (upper) and with a finger (lower). The numbers 1 to 5 refer to different designs as specified by Table II.

TABLE-II
PARAMETERS OF PRINTED MUTUAL CAPACITANCE SENSORS

sensor #	*designed dimensions*			*printed electrode width (µm)*
	Outer dimension (mm²)	*electrode width (µm)*	*gap width (µm)*	
1	7.70 x 9.70	150	750	112+-34
2	7.85 x 9.85	300	600	281+-32
3	8.00 x 10.00	450	450	440 +-35
4	8.15 x 10.15	600	300	610+-25
5	8.30 x 10.30	750	150	717

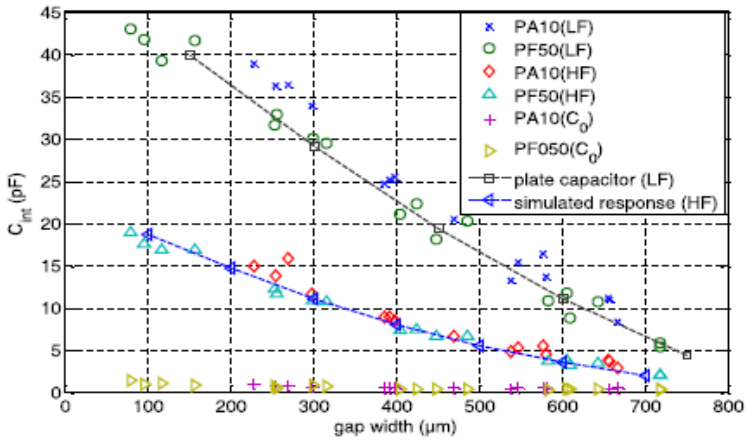

Fig.8. Response of printed mutual capacitance buttons to a drop of water in dependence on the gap between the electrodes. The low frequency (LF) response was evaluated at 1 kHz, the high frequency (HF) response at 1 MHz.

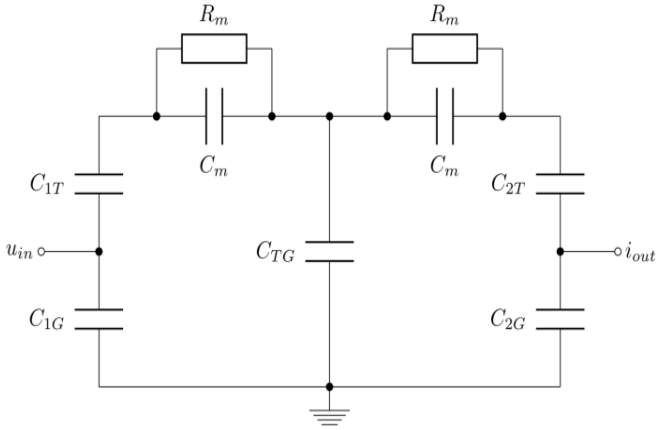

Fig.9. Equivalent circuit model of the mutual capacitance based touch sensor.

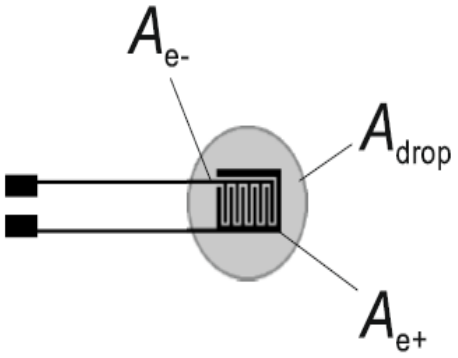

Fig.10. Illustration of the electrode areas of the capacitances occurring in the simplified LF equivalent circuit model.

In the high frequency limit, R_m can be neglected compared to C_m. Furthermore, the field distribution in the water drop is not uniform. The capacitance C_{TG} in the high frequency limit therefore is not linearly dependent on the drop area. To model the high frequency behavior of mutual capacitance, C_m and C_{TG} which are both unknown, are combined to C_m' and the high frequency model simplifies to a series connection of C_{1T}, C_{2T} and C_m'. The dependence of C_m' on the dimension of the sensor is further discussed in the simulations below.

The influence of the finger on the mutual capacitance of the sensor, over the whole considered frequency range, resembles the high frequency limit of the interaction with water. It can be concluded that, first, the relative permittivity of the finger for the given application can be approximated by the permittivity of water. Second, the specific conductivity of the finger is lower than the specific conductivity of the used deionized water. Otherwise, a stronger frequency dependence would occur.

With the simple LF model described above, excellent agreement between theoretical values and experiment was achieved. The results strongly depend on the estimated printed geometries. The uncertainties of layer thicknesses, electrode and drop areas are too high to validate the model more accurately. Therefore, 2D simulations were performed to further verify the consistency of the model.

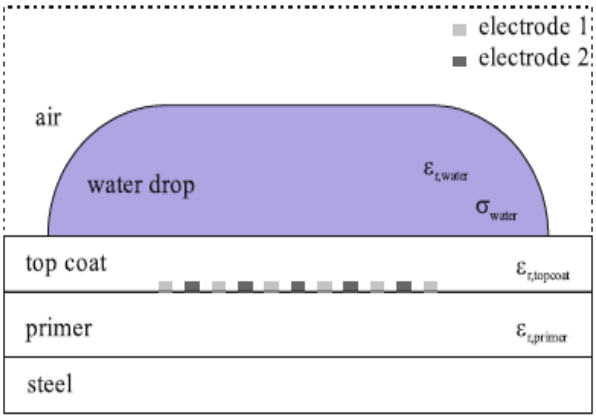

Fig.11. Schematic description of the simulated 2D structure. For better visibility, top coat, primer and electrodes are scaled by a factor of 100 in vertical direction.

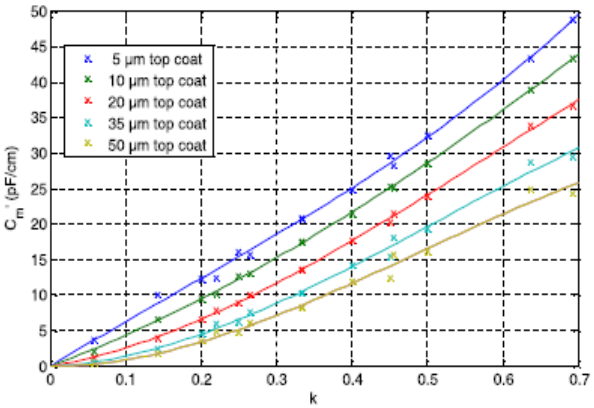

Fig.12. Simulated coupling capacitance C_m' in dependence on the design parameter k.

C. Mutual Capacitance: Simulations

Frequency dependent simulations of the mutual capacitance were performed with the AC/DC electric current module of COMSOL Multiphysics. The interdigital structure of the printed sensor was approximated by parallel infinitely long rectangular beams, embedded between two dielectric layers (compare Fig. 11). A drop of deionized water, fully covering the embedded electrodes, is situated on the top coat. For the deionized water, a relative permittivity of 80 and a specific conductivity of 19 µS/cm were assumed. The relative permittivity of the top coat and primer are 6.0 and 5.2, respectively. The steel substrate is defined as ground potential. Electrode 1 and electrode 2 are connected to different terminals. The potential of electrode 2 is set to zero (to mimic the virtual ground at the input of a transimpedance amplifier). A frequency dependent simulation ranging from 1 kHz to 1 MHz is performed. The gap size w_{gap} and the electrode width are both varied between 100 µm and 800 µm in the performed simulations.

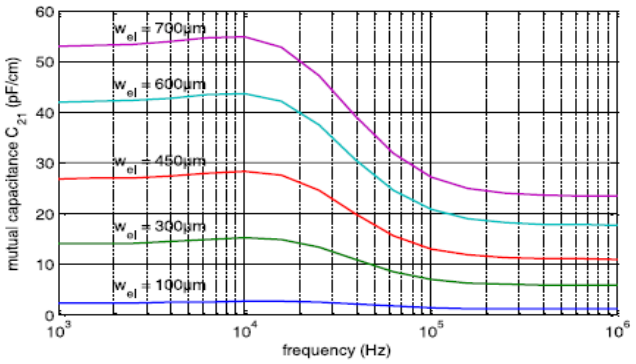

Fig.13. Simulated mutual capacitance of an interdigital sensor in contact with a drop of deionized water. The raster width, defined as the sum of electrode and gap width is 900 µm.

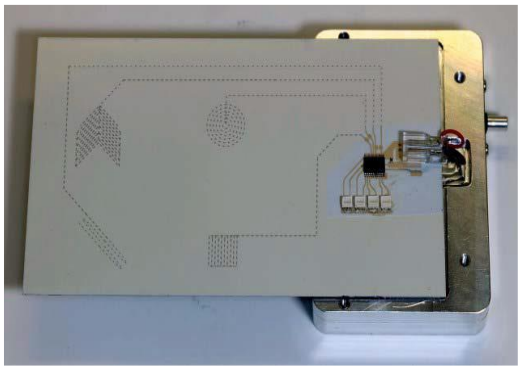

Fig.14. Capacitive sensors embedded in the organic coating of sheet steel. Sensor readout is realized with a dedicated MSP430 microcontroller which is mounted on the printed silver lines. The embedded capacitive sensors are indicated by dashed lines.

As an example, the simulated frequency dependent mutual capacitance $C_{21,sim}$ obtained with constant raster width $w_{raster} = w_{gap} + w_{electrode} = 900\ \mu m$ is depicted in Fig. 13. It clearly resembles the experimentally observed behavior(see also Fig. 7). The mutual capacitance is specified in dependence on the length of the interdigital structure. The simulated low frequency limit of $C21,sim$ was compared to the simplified plate type capacitor model (PTCM). For all simulated values, relative deviations below 0.5 % were obtained. In general, the capacitance was (slightly) underestimated with the PTCM. This can be expected, as the electric field between electrode and top surface, in general, will "spread" and therefore increase the effective area of the capacitive coupling and, consequently, the mutual capacitance.

Relations for the high frequency equivalent circuit capacitance C_m' can be obtained by 2D simulations. It is found that a reasonable approximation (compare Fig. 12) for the capacitance is given by:

$$C'_m(k,h) = a_3(h)\,k^3 + a_2(h)\,k^2 + a_1(h)\,k$$

Here, k is a dimensionless parameter $k = w_{el}/2/(w_{gap} + w_{el}/2)$, which is commonly used in the conformal mapping of coplanar waveguides, and h is the thickness of the topcoat.

The coupling capacitance C_m' was also simulated using the dimensions of the printed sensor structure. Assuming a sensor length of 5.5 mm, corresponding to the average effective length of the tines of the interdigital electrodes, the predicted response of the sensor is shown in Fig. 8, where excellent agreement between experimental and simulated values can be observed. It can be concluded, that the proposed method is suitable to model the response of mutual capacitance based sensors.

The response of interdigital sensors can be simulated with 2D models. The PTCM is suitable to predict the low frequency response of the sensor to water. To estimate the high frequency response to water and to the interaction with a finger, the coupling capacitance C_m' has to be simulated for the given design parameters.

V. Demonstator Devices

5.1. Coated Sheet Steel as Printed Circuit Board

A sensor panel with self-capacitance based sensors is printed with PF-050 silver ink on top of the 20 µm thick organic polyurethane based primer coating of a steel substrate (see Fig. 14). The conductor lines are 200 µm wide. To demonstrate the design freedom, different sensor shapes have been realized. Footprints for a MSP430G2x

microcontroller, dedicated for the readout of the sensors, and for multi-color LEDs are included in the printed structures. After being thermally cured at 140°C for 10 min, a 17 µm thick polyester top coat layer is applied to the printed structure by spin coating. The footprints are protected with adhesive tape which is removed after the spin coating sequence but prior to thermal curing of the top coat layer. The MSP430 and the LEDs are attached to the footprints with PF-050 silver ink. To supply the circuitry, the microcontroller is connected to a 3.0 V battery pack. All buttons are fully functional. With an appropriate choice of detection thresholds, the microcontroller can also distinguish between light and strong key strokes. Of course, the button itself is not force sensitive, but if a higher force is applied to the button, the effectively covered sensor area, and hence the self-capacitance increases.

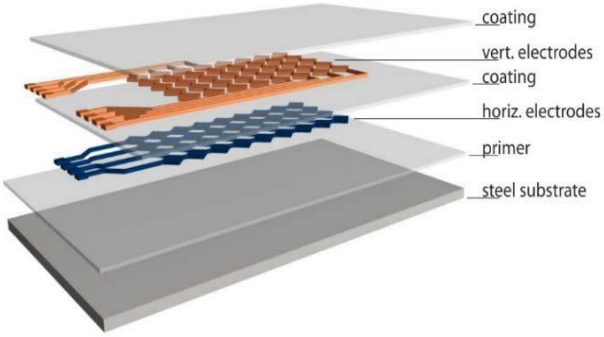

Fig. 15. Schematic layout of the touchpad.

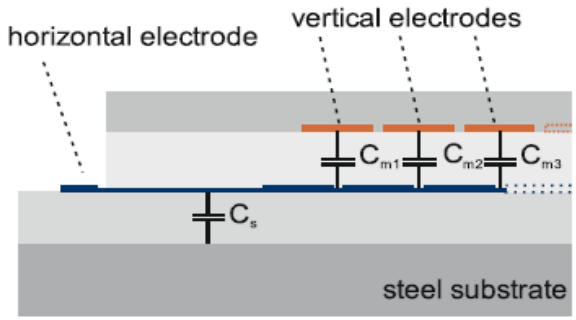

Fig. 16. Schematic cutout of the touchpad's side view illustrating the self capacitance C_s of the horizontal electrode and its mutual capacitance C_{mi} with three of the vertical electrodes.

5.2. Printed Touch Pad

As a second example for the device technology, a multilayer touchpad was fabricated (see Fig. 15). The electrodes were screen printed with a manual screen printing machine on a 20 µm thick polyurethane primer layer with PEDOT:PSS [8] ink. The intermediate and the top polyester coat layer were spin coated with layer thicknesses of 10 µm. The typical self-capacitance, i.e., the capacitance between electrode and ground (compare Fig. 17) of the vertical electrodes is in the order of 400 pF, for the horizontal electrodes it is about 650 pF. By interaction with a fingertip, the capacitances increase by typically 50% (vertical) and 11% (horizontal). Despite the large offset due to the proximity to the substrate, user interactions can be well detected. The mutual capacitance between horizontal and vertical electrodes (compare Fig. 16) is in the range of 5 pF. By application of a finger over a pad, it increases by a factor of 10.

VI. Conclusion

It was shown that coated sheet steel can be used as a substrate for printed electronics. As an example, the implementation of embedded touch buttons and a touchpad with diamond shaped electrodes are presented. The sensitivity of self- and mutual capacitance based sensors to user interaction in dependence on design parameters is investigated. A higher sensitivity was achieved with mutual capacitance based buttons. Furthermore an appropriate equivalent circuit model for embedded mutual capacitance based sensors was identified. Simulations have been performed, leading to a simplified relation which can be used to estimate the influence of user interaction (or water) on the mutual capacitance in dependence on the design parameters. In addition, it was shown that the low frequency interaction of water with mutual capacitance based sensors can accurately be described by a simplified plate-type capacitor based model. In general, the sensor response can be optimized by choosing a thick primer and a thin top coat layer in the design process. However, if a low primer thickness, e.g., due to costs reasons, is a prerequisite, or if a thick top coat, e.g., due to optical or protective reasons, is required, these boundary conditions are not an obstacle.

References

[1] S. Magdassi, M. Grouchko, O. Berezin, and A. Kamyshny, "Triggering the sintering of silver nanoparticles at room temperature," *ACS Nano*, vol. 4, no. 4, pp. 1943–1948, Apr. 2010.

[2] D. Huang, F. Liao, S. Molesa, D. Redinger, and V. Subramanian, "Plastic-compatible low resistance printable gold nanoparticle conductors for flexible electronics," *J. Electrochem. Soc.*, vol. 150, no. 7, pp. G412–G417, 2003.

[3] S.-H. Park and H.-S. Kim, "Flash light sintering of nickel nanoparticles for printed electronics," *Thin Solid Films*, vol. 550, pp. 575–581, Jan. 2014.

[4] J. Ryu, H.-S. Kim, and H. T. Hahn, "Reactive sintering of copper nanoparticles using intense pulsed light for printed electronics," *J. Electron. Mater.*, vol. 40, no. 1, pp. 42–50, Jan. 2011.
[5] S. B. Walker and J. A. Lewis, "Reactive silver inks for patterning high-conductivity features at mild temperatures," *J. Amer. Chem. Soc.*, vol. 134, no. 3, pp. 1419–1421, Jan. 2012.
[6] D. J. Finn, M. Lotya, and J. N. Coleman, "Inkjet printing of silver nanowire networks," *ACS Appl. Mater. Interfaces*, vol. 7, no. 17, pp. 9254–9261, Apr. 2015.
[7] *Electrodag PR-406B*, Henkel, Düsseldorf, Germany.
[8] *Orgacon EL-P 5015*, AGFA, Mortsel, Belgium.
[9] P. Kopola *et al*, "Gravure printed flexible organic photovoltaic modules," *Solar Energy Mater. Solar Cells*, vol. 95, no. 5, pp. 1344–1347, May 2011.
[10] P. Tehrani, L.-O. Hennerdal, A. L. Dyer, J. R. Reynolds, and M. Berggren, "Improving the contrast of all-printed electrochromic polymer on paper displays," *J. Mater. Chem.*, vol. 19, no. 13, pp. 1799–1802, Feb. 2009.
[11] M. Jung *et al.*, "All-printed and roll-to-roll-printable 13.56-MHzoperated 1-bit RF tag on plastic foils," *IEEE Trans. Electron Devices*, vol. 57, no. 3, pp. 571–580, Mar. 2010.
[12] F. C. Krebs *et al.*, "A complete process for production of flexible large area polymer solar cells entirely using screen printing-first public demonstration," *Solar Energy Mater. Solar Cells*, vol. 93, no. 4, pp. 422–441, Apr. 2009.
[13] *Geometrical Product Specifications (GPS)? Surface Texture: Profile Method? Terms, Definitions and Surface Texture Parameters*, document EN ISO 4287, 2009.
[14] Z. Kolská, A. ˇ Reznícková, V. Hnatowicz, and V. Švorcík, "Surface properties of poly (ethylene terephthalate) foils of different thicknesses," *J. Mater. Sci.*, vol. 47, no. 17, pp. 6429–6435, Sep. 2012.
[15] B. Trnovec *et al.*, "Coated paper for printed electronics," *Prof. Papermaking*, vol. 1, nos. 48–51, p. 104, 2009.
[16] A. Sandström, A. Asadpoordarvish, J. Enevold, and L. Edman, "Spraying light: Ambient-air fabrication of large-area emissive devices on complex-shaped surfaces," *Adv. Mater.*, vol. 26, no. 29, pp. 4975–4980, Aug. 2014.
[17] A. C. Hübler, M. Bellmann, G. C. Schmidt, S. Zimmermann, A. Gerlach, and C. Haentjes, "Fully mass printed loudspeakers on paper," *Organic Electron.*, vol. 13, no. 11, pp. 2290–2295, Nov. 2012.
[18] D. Tobjörk and R. Österbacka, "Paper electronics," *Adv. Mater.*, vol. 23, no. 17, pp. 1935–1961, May 2011.
[19] T. H. J. van Osch, J. Perelaer, A. W. M. de Laat, and U. S. Schubert, "Inkjet printing of narrow conductive tracks on untreated polymeric substrates," *Adv. Mater.*, vol. 20, no. 2, pp. 343–345, Jan. 2008.
[20] C. M. Hansen, *Hansen Solubility Parameters: A User's Handbook*. Boca Raton, FL, USA: CRC Press, Jun. 2007.
[21] F. Grasso, F. Musumeci, and A. Triglia, "Impedance spectroscopy of pure water in the 0.01 Hz to 100 kHz range," *Il Nuovo Cimento D*, vol. 12, no. 8, pp. 1117–1130, Aug. 1990.

